Measurement of the Ionospheric Scintillation Parameter C_kL From SAR Images of Clutter

David P. Belcher, Christopher R. Mannix, and Paul S. Cannon

***Abstract*— Space-based synthetic aperture radar (SAR) can be affected by the ionosphere, particularly at L-band and below. A technique is described that exploits the reduction in SAR image contrast to measure the strength of ionospheric turbulence parameter C_kL. The theory describing the effect of the ionosphere on the SAR point spread function (PSF) and the consequent effect on clutter is reviewed and extended. This theory can then be used to determine C_kL from both corner reflectors (CRs) and K-distributed SAR clutter. Measuring the K-distribution order parameter allows C_kL values much lower than those that defocus the image to be determined. The results of an experiment in which a CR on Ascension Island was repeatedly imaged by PALSAR-2 in the spotlight mode during the scintillation season are described. The value of C_kL obtained by measuring the clutter was compared with that obtained from a nearby CR. The correlation between the two was good using a median value of the spectral index p. This correlation was improved by using the measured value of p derived from the CR PSF. The technique works for any homogeneous K-distributed SAR clutter and is thus applicable to extra-terrestrial bodies as well as PALSAR-2 images of Ascension Island.**

***Index Terms*— Ionosphere, ionospheric electromagnetic propagation, synthetic aperture radar (SAR).**

I. Introduction

A. Background

THE ionosphere has a number of effects on a space-based synthetic aperture radar (SAR) operating at L-band and lower frequencies, such as Faraday rotation [1], [2], image geometric distortion [3], phase shift and defocusing [4], amplitude modulation [5], [6], and loss of contrast [7].

Previous work [8] has shown that the primary effect of phase scintillation is to induce an along-track point spread function (PSF) that is dependent on the scintillation parameters. Two of the most important are C_kL, the integrated strength of ionospheric turbulence at 1-km scale size, and p, the spectral index of the ionospheric phase screen.

Measurement of the PSF therefore allows both of these parameters to be determined directly from the PSF [9]. Comparison of this method of measuring $C_{\mathbf{k}}L$ with a more conventional method using GPS receivers shows that the two are strongly correlated [10]. The main limitation in the comparison is the differing time and spatial scales of GPS spectra and SAR apertures [10]. Using the PSF to measure $C_{\mathbf{k}}L$ is, however, only possible in locations where there are corner reflectors (CRs). This is a severe restriction and consequently measuring C_kL using only clutter is desirable.

The effect of this ionosphere-induced PSF is to reduce the image contrast, an effect that occurs at C_kL values that are much lower than those that will defocus the image. For SAR clutter that is K-distributed, this loss of contrast is more appropriately described by a rise in the K-distribution order parameter, which is a more accurate measure. It can be shown that the rise in the order parameter is directly proportional to $C_{\mathbf{k}}L$ using both theory and simulations [7]. Thus, by measuring the rise in the order parameter, $C_{\mathbf{k}}L$ can be determined. This forms the basis for the technique described and tested in this paper.

The order parameter value is a property of the terrain and clutter type, and varies from one location to another [11]. It is therefore not possible to measure the rise in the order parameter using only one SAR image. However, measuring the order parameter of two SAR images of the same place, one with ionospheric effects, and one without, allows the rise in the order parameter due to the ionosphere to be determined.

An experiment has been conducted that repeatedly imaged Ascension Island using PALSAR-2 [12] in the spotlight mode at high resolution (1 m) during the scintillation season [9]. The imagery from this experiment provides an excellent test of this method, since the imagery includes both CRs and clutter.

In the following section, the theory of ionospheric effects on the PSF and clutter is reviewed and then extended to cover all synthetic aperture lengths and all values of p. In Section III, the comparison between the clutter and CR methods are described and applied to the experimental PALSAR-2 data. Finally, conclusions are drawn in Section IV.

II. Theory

A. Point Spread Function

Turbulence in the ionosphere causes irregularities in electron density, which in turn causes fluctuations in the phase of a radar signal passing through it. These fluctuations, known as scintillation, can be related to the turbulence of the irregularities using weak scattering theory [13]. The phase scintillation raises the level of along-track sidelobes, and if severe enough, cause defocusing. For an L-band SAR, such as PALSAR-2, ionospheric effects are often observed, but complete defocusing is very rare.

The phase fluctuations, although random, have a spectrum that is characteristic of the turbulent conditions in the ionosphere. The phase power spectrum can also be related to the shape of the SAR sidelobes [8]. Although the sidelobes

Manuscript received August 29, 2016; revised December 16, 2016 and April 11, 2017; accepted May 15, 2017. Date of publication August 8, 2017; date of current version September 25, 2017. This work was supported by the U.K. Engineering and Physical Sciences Research Council under Grant EP/I013601/1. *(Corresponding author: David P. Belcher.)*

The authors are with the University of Birmingham, Birmingham B15 2TT, U.K. (e-mail: d.belcher@bham.ac.uk).

Color versions of one or more of the figures in this paper are available online at http://ieeexplore.ieee.org.

Digital Object Identifier 10.1109/TGRS.2017.2717081

are random, their ensemble average shape can be described by a PSF. The ionospherically disturbed PSF is equal to the mainlobe (given by the Fourier transform of the amplitude weighting) plus the sidelobes. Provided that the amplitude weighting is chosen to produce a delta-like PSF in the absence of scintillation, these sidelobes will be dominated by the phase power spectrum and hence will be characteristic of the ionospheric turbulence. The sidelobe function (SLF) due to scintillation is given by [7]

$$\langle|\eta(r^{/})|^2\rangle = T_{\mathrm{SLF}}\left(\sqrt{r_0^2+(|r^{/}|+1)^2}\right)^{-p} \tag{1}$$

where $\langle|\ |^2\rangle$ denotes the ensemble average intensity, T_{SLF} is the turbulence of the sidelobes (and can be related to many other ionospheric parameters), $r^{/}$ is the along track resolution cell and p is the ionospheric phase screen spectral index.

The parameter $r_0 = L_{\mathrm{SA}}/\gamma\, l_0$ is the ratio of the synthetic aperture length L_{SA} to the ionospheric outer scale size l_0 scaled by γ, the velocity ratio of the satellite to the effective velocity of the ray path in the phase screen. In general, r_0 can be determined from the imaging geometry and resolution using the method of Belcher and Cannon [5] to determine γ, but T_{SLF} and p are properties of the ionosphere which vary from one imaging pass to the next.

Note that in the above, the center of the mainlobe occurs at $\boldsymbol{r}^{/} = 0$. It is often convenient to redefine the center of the mainlobe to be at $\boldsymbol{r} = 1$ and use the fact that $\langle|\eta(\boldsymbol{r}^{/})|^2\rangle$ is an even function so that measurements of $|\eta(\boldsymbol{r})|^2$ can be plotted as a function of $\log r$. (Hence resolution cell $r = |r^{/}| + 1$.)

The value of T_{SLF} is given by [7]

$$T_{\mathrm{SLF}} = \frac{4\gamma\,\kappa_C^{1-p} G \sec\theta (r_e\lambda_0)^2\sqrt{\pi}\,\Gamma(p/2)}{(2\pi)^2\Gamma((p+1)/2)\kappa_{1\mathrm{km}}^{-1-\mathrm{p}}} C_k L \tag{2}$$

where $\kappa_C = 2\pi\,\gamma\,/L_{SA}$, G is a geometric enhancement factor that is unity in an isotropic ionosphere, θ is the incidence angle to the ionosphere, r_e is the classical electron radius, λ_0 is the wavelength at the radar center frequency, $\kappa_{1\mathrm{km}} = 2\pi/1000$, and $C_k L$ is the integrated strength of ionospheric turbulence at 1-km scale size.

The effect of raised sidelobes on a point target, such as a CR is most visible when both the resolution and radar cross section (RCS) of the target are high. An example of a PSF that has been disturbed by the ionosphere is shown in Fig. 1. This PSF is from a 47-dBm^2 CR on Ascension Island imaged with PALSAR-2 at 1-m resolution [9]: the left and right halves of the PSF have been averaged to produce a single-sided plot. The ensemble average shape of the sidelobes (SLF) has been fitted to the measured CR, from which a value of T_{SLF} and p can be obtained.

Given a measurement of T_{SLF} and p, (2) can be used to determine $C_k L$, since all the other parameters can either be determined from the geometry or estimated from a climatological model such as WBMOD [14]. Thus, given a measurement of p and T_{SLF}, the value of $C_k L$ can be measured, as shown in Fig. 1.

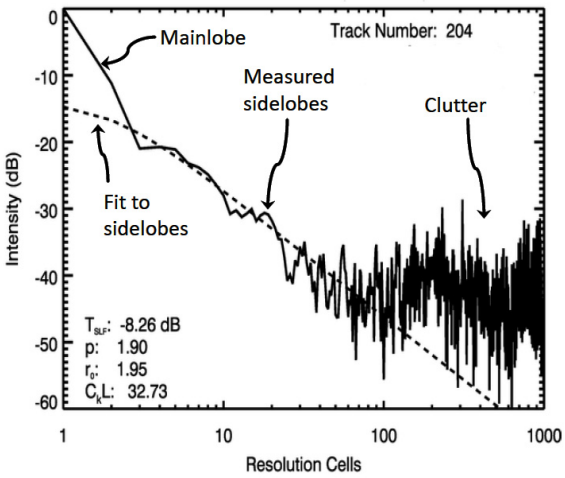

Fig. 1. Ionospherically disturbed PSF obtained on February 5, 2015.

B. Correlated K-Distributed Clutter

One of the simplest and most effective models of radar clutter is the correlated K-distributed model [11], [15], [16]. In this model, the observed clutter results from the product of the underlying radar cross section (which is generally correlated over a few resolution cells) with uncorrelated complex Gaussian speckle. The underlying cross section is assumed to be gamma-distributed in intensity, so that when combined with the speckle, the image statistics have a K-distributed intensity. The K-distribution is an excellent fit to natural clutter [16] and has just two parameters, the mean μ and order parameter ν.

The order parameter ν can be estimated using natural logs via [17]

$$\nu = \left[\frac{\langle I\log I\rangle}{\langle I\rangle} - \langle\log I\rangle - 1\right]^{-1} \tag{3}$$

where each pixel is of intensity I.

The effect of raised sidelobes is to add random complex Gaussian noise to the image. Thus the speckle, which is nominally of unit variance, increases. The total power in the sidelobes, as measured by the variance, is

$$\sigma_{\mathrm{SLF}}^2 = \int_{-\infty}^{\infty} |\eta(\boldsymbol{r}^{/})|^2 dr^{/}. \tag{4}$$

Convolving the image that would have been obtained in the absence of ionospheric disturbance with the ionospherically induced PSF therefore increases the speckle variance to $1+\sigma_{\mathrm{SLF}}^2$. The mainlobe power is reduced by the leakage into the sidelobes, so the effective mean of the underlying cross section is also reduced by the same amount.

At the same time, the variation in the underlying cross section is smoothed out by the PSF. The PSF effectively adds together samples of the gamma-distributed cross section (which is correlated over l_r resolution cells) by an amount that depends on the sidelobe shape. The addition of independent gamma-distributed samples does not affect the mean, but increases the order parameter in proportion to the effective number of independent samples. The ionospherically disturbed order parameter ν_d is therefore given by [7]

$$\nu_d = \nu\left(1+\sigma_{\mathrm{SLF}}^2/l_r\right). \tag{5}$$

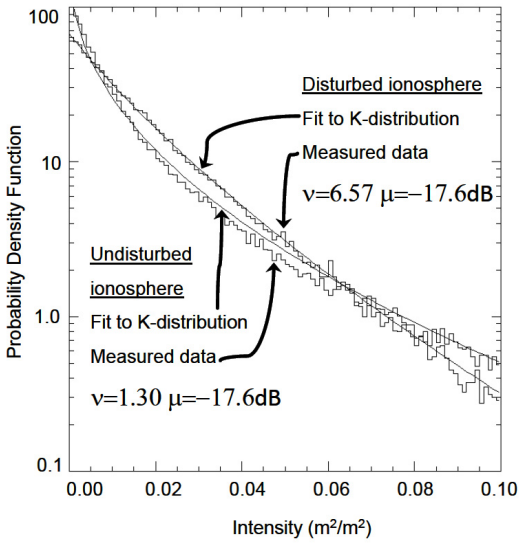

Fig. 2. Effect of the ionosphere on clutter with a K-distributed pdf (histogram: experimental data; solid line: fit to theory).

When the increase in the speckle power and increase in the order parameter of the underlying gamma-distributed cross section are combined in the product model, it is found that the statistics remain K-distributed, but with order parameter ν_d and unchanged mean [7].

An example of the effect of the ionosphere on the clutter probability density function (pdf) is shown in Fig. 2 using experimental data from part of a PALSAR-2 image of the west side of Ascension Island. The undisturbed image was obtained on August 18, 2014, before the start of the scintillation season, and the disturbed image was obtained on October 27, 2014. Details of the experiment are given in Section III.

As can be seen, the K-distribution is a good fit to the experimental data, the deviations in the intensity of the undisturbed clutter from the fit is almost certainly the result of some inhomogeneity in the image. The increasingly noisy histogram at the higher intensities is due to the limited number of high intensity pixels for a small image size. The ionospheric disturbance has increased the order parameter from 1.30 to 6.57, and has actually reduced the deviation from the K-distribution, probably due to the smoothing effect of the PSF. It is clear that the pdf remains K-distributed after ionospheric disturbance, but with a higher order parameter as predicted [7].

The correlation distance in resolution cells l_r relates to the correlation of the underlying terrain, not the speckle, and can be obtained from the intensity autocorrelation function (ACF) [7], [11]. Measuring the order parameter ratio between an ionospherically disturbed and undisturbed SAR image, therefore, allows the value of σ^2_{SLF} to be estimated. This process will obviously be more accurate if both ν and l_r are small: if either is infinite (pure speckle) the effect cannot be detected and σ^2_{SLF} cannot be measured. Since larger resolution cells have more scatterers in them, larger resolutions tend to be closer to negative-exponentially distributed speckle and therefore have both large order parameters and large correlation lengths. Thus for the most accurate measurements of σ^2_{SLF} high-resolution imagery is required.

C. Determining $C_k L$ From σ^2_{SLF}

The total power in the sidelobes is given by the integral over the double-sided SLF. The finite length of the SLF is N_{SA}, the number of independent samples in the synthetic aperture. The total sidelobe power is therefore

$$\sigma^2_{\mathrm{SLF}} = 2T_{\mathrm{SLF}} \int_1^{N_{\mathrm{SA}}/2} \left(\sqrt{r_0^2 + r^2}\right)^{-p} dr. \tag{6}$$

This integral has no exact analytic solution, but by making appropriate approximations, a good solution can be found. For example, $N_{\mathrm{SA}} \gg r_0$ and N_{SA} can usually be considered infinite.

When $r_0 \ll 1$ (or equivalently when $L_{\mathrm{SA}} \ll \gamma\, l_0$) then the square root term may be approximated by r^{-p} and

$$\sigma^2_{\mathrm{SLF}} = \frac{2T_{\mathrm{SLF}}}{p-1}. \tag{7}$$

When r_0 is not sufficiently small that it can be neglected, the total sidelobe power can be expressed as

$$\sigma^2_{\mathrm{SLF}} = 2T_{\mathrm{SLF}} \int_0^{\infty} \left(\sqrt{r_0^2 + (r+1)^2}\right)^{-p} dr. \tag{8}$$

This integral also cannot be solved, except when $r_0 \gg 1$ (or equivalently $L_{\mathrm{SA}} \gg \gamma\, l_0$) so that the terms inside the square root can be approximated to $r_0^2 + r^2$, in which case

$$\sigma^2_{\mathrm{SLF}} = T_{\mathrm{SLF}} r_0^{1-p} \frac{\sqrt{\pi}\,\Gamma((p-1)/2)}{\Gamma(p/2)}. \tag{9}$$

These two cases, the large r_0 and small r_0 case, may be combined into a single equation. Substituting for the value of T_{SLF} (2) then, in both cases the total sidelobe power may be expressed as

$$\sigma^2_{\mathrm{SLF}} = 8\pi\, \gamma^{2-p} G \sec\theta (r_e \lambda_0)^2 \frac{c_p}{p-1} 10^{-6} L_{\mathrm{km}}^{p-1} C_k L \tag{10}$$

where c_p is a parameter that depends only on p, typical values for which are $1 \le p < 4$, corresponding to $1 \ge c_p > 0.4$. The value of c_p and L_{km} depend on the relative lengths of the synthetic aperture and the effective outer scale $\gamma\, l_0$, as follows:

$$\begin{aligned} L_{\mathrm{SA}} \gg \gamma\, l_0 &\begin{cases} L_{\mathrm{km}} = \gamma\, l_{0\_\mathrm{km}} \\ c_p = 1 \end{cases} \\ L_{\mathrm{SA}} \ll \gamma\, l_0 &\begin{cases} L_{\mathrm{km}} = L_{\mathrm{SA\_km}} \\ c_p = \frac{\Gamma(\mathrm{p}/2)}{\sqrt{\pi}\,\Gamma((p+1)/2)}. \end{cases} \end{aligned} \tag{11}$$

The value of σ^2_{SLF} from both the large and small r_0 approximations are exactly equal for $p = 2$ when $L_{\mathrm{SA}} = \frac{\pi}{2}\gamma\, l_0$ and, for $p = 3$, when $L_{\mathrm{SA}} = \sqrt{2}\gamma\, l_0$. In practice, for the median p, the breakpoint occurs at $r_0 \approx 1.5$. Thus (10) represents a good solution to the integral (6) provided that below this point, L_{km} is equal to $L_{\mathrm{SA\_km}}$, and above it by limiting L_{km} to $\gamma\, l_{0_{\mathrm{km}}}$. At this point, L_{km} no longer depends on the synthetic aperture length, and σ^2_{SLF} is therefore independent of the resolution.

In the special case of $p \to 1$, the sidelobe integral (10) tends to infinity, but in reality the finite length of the PSF comes back into play and (6) must be used with $p = 1$. Performing this integration also results in (10) but with the $(p-1)^{-1}$ term limited to be no greater than $\ln N_{\mathrm{SA}} - \ln(1+(r_0^2+1)^{1/2})$. Thus

for a typical $N_{SA} = 10\,000$, and $r_0 = 3$, this is equivalent to limiting $p > 1.128$ in the $(p-1)^{-1}$ term. Values of $p < 1$ are nonphysical and do not occur in the ionosphere.

All the parameters in (10) are known, or can be estimated from WBMOD [14], except $C_k L$ and p, so measureing σ^2_{SLF} and p allows $C_k L$ to be determined. Unfortunately, the value of p cannot currently be estimated from the clutter, so the median value of $p = 2.5$ has to be used.

For the experimental PALSAR-2 data used in this paper, the value of r_0 is between 1 and 6, so $c_p = 1$ and $L_{km} = \gamma\, l_0/1000$. The sensitivity of (10) to an assumed median value can be estimated using values of $p = 2$ and $p = 4$, for a typical value of $L_{km} \approx 10\gamma$. This results in a $\log_{10} C_k L$ error $\sim$1.5, which, although significant is useful given the large dynamic range of $C_k L$. Since the overwhelming majority of p values lie between 2 and 3 [18], the typical error will be less than this.

Although the value of p cannot currently be determined from the image intensity, by substituting the PSF $h(r) = \delta(r) + \eta(r)$ into the form of the intensity ACF derived in [11] and evaluating the integrals, and neglecting the products of two sidelobe intensity terms, it is possible to re-expresss the ACF as the sum of two spatially invariant double convolutions [7], [19]. By taking the Fourier transform of the result, it can be shown that the spectrum of SAR image intensity is approximately equal to the spectrum of the speckle intensity plus the spectrum of PSF intensity divided by the order parameter, plus the spectrum of the underlying cross section multiplied by the spectrum of $|h(r)|^2$ also divided by the order parameter. This offers the possibility of determining p from the clutter intensity image, but is beyond the scope of this paper.

III. Experimental Data

A. Experiment Description

The design and conduct of the experiment are described in detail in [9]. The experiment essentially involved repeatedly imaging two CRs on Ascension Island using PALSAR-2 [12] in the spotlight mode. The island is located in the mid-Atlantic under the ionospheric equatorial anomaly.

One CR was located on the east side of the island and looked east, and the other was located on the western side of the island and looked west, thus allowing imaging from either direction. Since the CR RCS was approximately 47 dBm^2, and the resolution in the along-track direction was 1 m, the PSF can be very accurately measured.

During the scintillation season from September 2014 to March 2015, a total of 76 images were collected. Many of the collected images showed the effects of scintillation, and by fitting the theoretical shape of the PSF to the measured PSF, the values of T_{SLF} and p were determined. Since T_{SLF} can be directly related to $C_k L$ using (2), this allowed the value of $C_k L$ to be measured [9], [10].

Ascension Island experiences little seasonal variation in weather, being located just 8° south of the equator. The terrain was therefore assumed to be temporally invariant during the experiment. Provided that homogeneous areas were selected, this terrain was found to be a very good fit to the K-distribution model described above. This allows the order parameter to be accurately determined, and by selecting scintillation free days as a reference, the order parameter ratio, and hence σ^2_{SLF}, can be calculated.

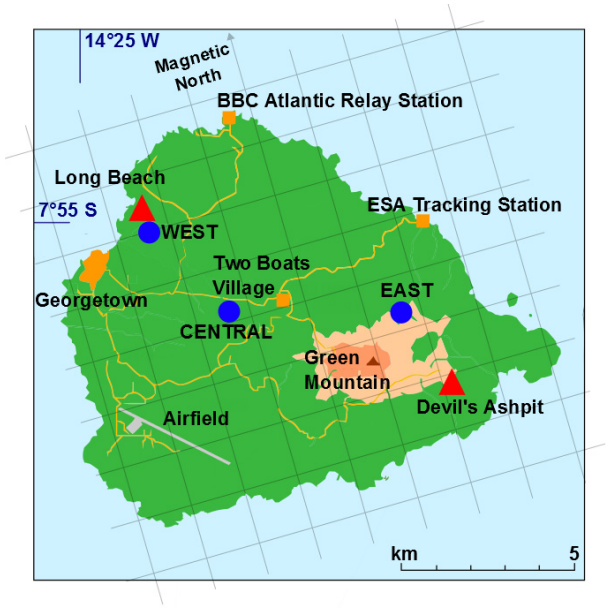

Fig. 3. Map of Ascension Island, showing the clutter areas (circles) and CRs (triangles).

B. Clutter Area Selection

Three areas of homogeneous terrain were selected, one near the west-CR, one near the east-CR, and one in the center of the island. The locations of these homogeneous areas on Ascension Island are shown in Fig. 3 by circles and the trihedral CRs by the triangles.

In this context, homogeneous terrain means an image area that can be completely represented by: 1) stationary single point statistics, comprised of a single K-distribution and 2) a constant spatially invariant ACF. Examples of such terrain can include natural rainforest or regularly spaced orchards, but not their boundary edges or changes in tree spacing. On Ascension the terrain is largely volcanic mixed with thorn bushes.

Fig. 4 shows the west area of Ascension Island imaged with PALSAR-2 before the start of the scintillation season. The distinctive "+" shape of the CR can be seen at the top, horizontally centered, and the clutter area is shown by the box. This area is relatively homogeneous, but not perfectly so.

The clutter areas selected were all of size 200 by 200 resolution cells. The sampling rate was doubled in the along-track direction using a zero-padded Fourier transform of the complex data, so that the intensity image remained Nyquist sampled. The location of the three clutter areas and their relative distance from the CRs are shown in Table I. Each area was extracted from the full image using its position relative to the CR, which ensures that the same area of ground can be compared.

The size of the clutter area on the ground changes with incidence angle since the range resolution relates to slant

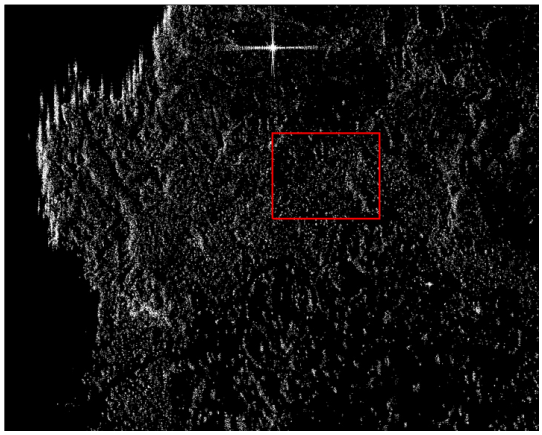

Fig. 4. West-clutter area (box) and CR (August 18, 2014).

TABLE I
LOCATIONS OF CLUTTER AREAS ON ASCENSION ISLAND

Clutter location	Position of bottom left corner (latitude, longitude)	Distance to	
		West-CR	East-CR
West	-7.916414, 14.400222	312 m	9170 m
Central	-7.939600, 14.375635	4041 m	5685 m
East	-7.929528, 14.336634	7407 m	2963 m

range and not ground range. Thus the resolutions of the image are 1 m (along track) and 1.78 m (slant range). An example of one of the clutter areas collected at an incidence angle of 69.7° is shown in Fig. 5, the range direction being horizontal. As can be seen, the effect of the ionosphere is to reduce the contrast of the image and smooth out the underlying cross section.

C. Comparison of Clutter and CR Measures of σ^2_{SLF}

The characteristics of the clutter (such as the order parameter and correlation length) are strongly dependent on the incidence angle. Thus to determine the order parameter ratio, two images of the same area obtained from the same satellite position are required. The undisturbed image of the pair was selected as the one having the lowest average order parameter, the assumption being that this is the undisturbed image.

Images for which the measured $p > 5$ have ionospheric effects that are too small to be measured and were therefore excluded from the set of disturbed images. It was also found that images with incidence angles of less than 30° did not produce good results. This was probably due to the much reduced CR RCS and much higher clutter, making accurate measurement of the CR sidelobes difficult. These images were therefore also excluded from the analysis.

The correlation length l_r was measured by fitting the theoretical shape [7], [11] to the ACF. The ACF region between 2.5 and 10 resolution cells was used for the fitting, to avoid the mainlobe (<2.5) and noise effects (>10). Amplitude scintillation effects on the SAR imagery were not observed at Ascension Island and no correction for amplitude scintillation was applied [5], [6].

Fig. 6 shows the comparison between the value of σ^2_{SLF} derived from the order parameter ratio (5) and that obtained

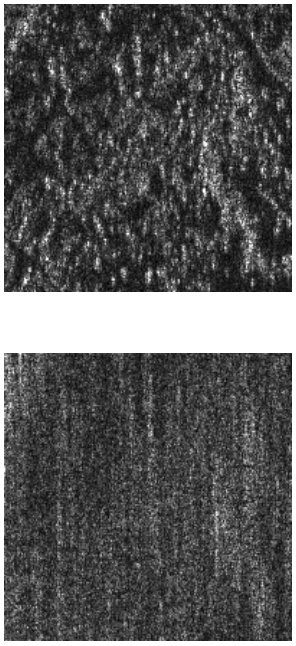

Fig. 5. West-clutter area. (Top) Undisturbed (August 18, 2014). (Bottom) Disturbed (October 27, 2014).

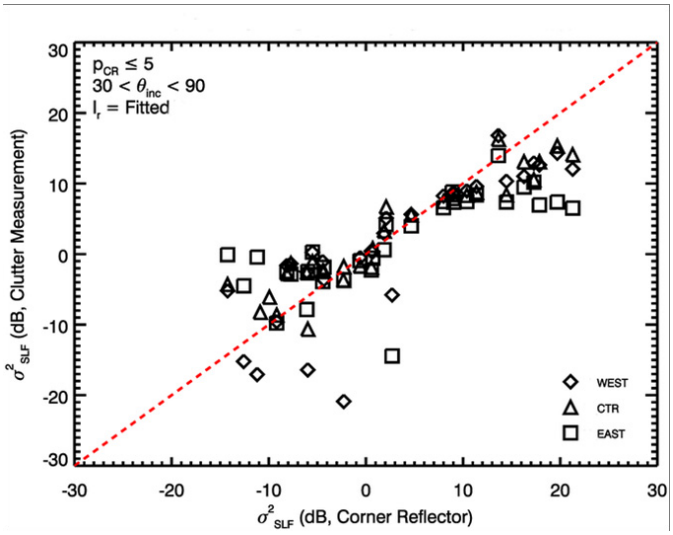

Fig. 6. Comparison of σ^2_{SLF} from order parameter and CR.

from the CR. (The CR values of σ^2_{SLF} were derived from the fit values of T_{SLF} and p.) As can be seen, the correlation between the two methods of measuring σ^2_{SLF} is excellent. This remains true even for very high values of σ^2_{SLF} where the images are defocused.

Including the value of l_r is important to ensure that the clutter measure does not underestimate σ^2_{SLF}. The intercept of Fig. 6 is within 0.5 dB of zero, which would not have been the case without including l_r. In general, the correlation lengths l_r are similar for the west- and central-clutter areas, but longer for the east-clutter area. As can be seen, the spread of values is slightly greater for the east-clutter area than the other two. Thus a shorter correlation length is desirable for accurate measurement of σ^2_{SLF}.

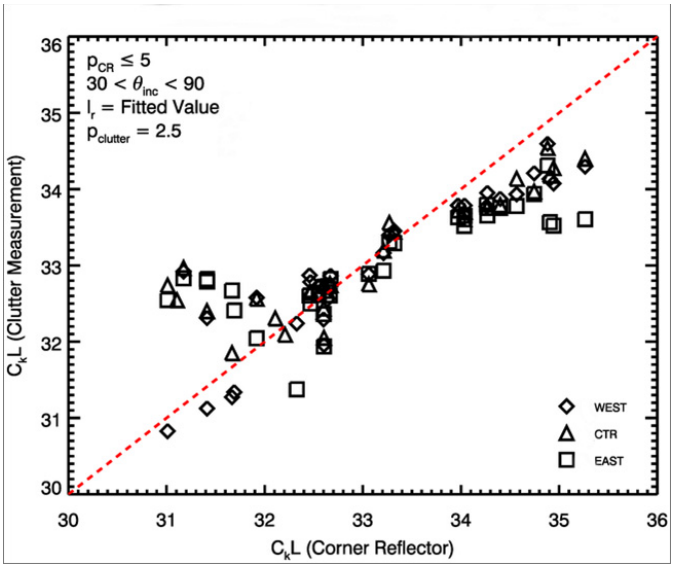

Fig. 7. Comparison of C_kL from CR and clutter (median p).

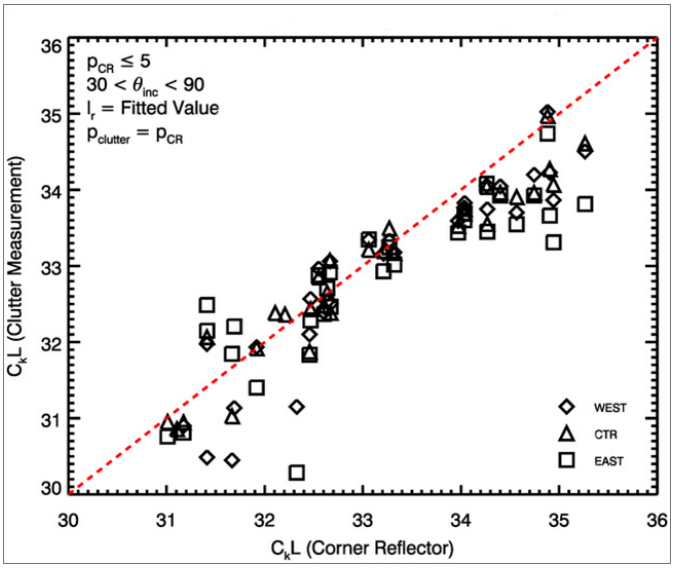

Fig. 8. Comparison of C_kL from clutter and CR (both using p from the CR).

D. Comparison of Clutter and CR Measures of C_kL

The value of σ^2_{SLF} is not useful in itself, but can be used with (10) to derive C_kL. The estimated values of G and γ can be determined from the irregularity elongation model [14] for Ascension Island, as described in [5]. An outer scale size of 10 km was assumed with this elongation model, the parameters of which are stable. Unfortunately, p is not stable, but varies considerably from pass to pass, and the median value of $p = 2.5$ has to be assumed. The results of comparing the value of C_kL determined in this manner with those from the CR are shown in Fig. 7.

As can be seen, the correlation between the two measures of C_kL is good, but the clutter measure shows less variation than the CR measure. The effect of the lack of knowledge of p can be determined by using the value of p from the CR (the "correct" value of p) in the clutter calculation of C_kL. This is shown in Fig. 8.

The overall correlation in Fig. 8 between the two methods (clutter and CR) of deriving C_kL is 0.95. The lowest correlation obtained, using only the east-clutter area, is 0.91. The slope of the fit between the two measures is 1, 0.83, and 0.72 for the west-, central-, and east-clutter areas, respectively.

If the results from the east-CR are removed from the data set, so that each clutter area always has the same distance from the remaining west-CR, the correlation improves. Furthermore, the closer the clutter area is to the west-CR, the better the correlation between the two measures of C_kL. Thus the differences between the clutter and CR measures are probably due to the distance between the CR and clutter area. Unfortunately, there are not enough points to establish the reverse correlation for the east-CR, since it contributes less than 20% of the data points. This is consistent with other results [10] which show that C_kL can vary over relatively small distances.

It is worth commenting that although knowledge of p produces a more accurate result (the correlation between the clutter and CR measures is better in Fig. 8 than Fig. 7), the measure is still useful when the median value is used, as shown in Fig. 7. This result is not unexpected since the overwhelming majority of p values are between 2 and 3 [18], thus justifying the use of the median value of 2.5. However, an independent measure of p obviously improves the accuracy.

IV. Conclusion

The PALSAR-2 spotlight imagery of Ascension Island, collected during the scintillation season near the peak of the sun-spot cycle, has proved to be ideal for measuring scintillation effects on SAR. Using these data, it is possible to measure the effect of phase scintillation by measuring the K-distribution order parameter. By using a CR to measure C_kL over almost the same temporal and spatial scale as that used to image the clutter, it is possible to verify the method. This shows that the order parameter ratio is a simple and effective means of determining the ionospheric turbulence.

The main limitation of determining C_kL from the clutter is that the value of p is unknown and has to be determined by another method. The order parameter ratio method would obviously benefit from a measure of p from the clutter itself.

The value of C_kL determined from the clutter is, on average, less than that determined from the CR when C_kL is high. This may be due to the spatial variation of C_kL since the size of the effect depends on the distance from the CR and is not obviously clutter texture dependent. The method appears to be robust, tolerating some inhomogeneity and continues to work under defocusing.

The total amount of noise introduced into the image by the ionospheric turbulence is proportional to σ^2_{SLF} and reducing this will be an important part of an autofocus technique. The criterion for an optimally focused SAR image is therefore that of minimum order parameter.

The order parameter ratio method can be applied to any SAR imagery that is K-distributed. Since Ascension Island is largely volcanic, this probably means that the technique can be applied to a number of other nonterrestrial bodies.

Although Ascension Island did include some vegetation growing amongst the regolith, the vegetation is sparse. The

technique has yet to be tested on a wider variety of terrain, such as rainforest, or on terrain that experiences strong seasonal variation.

The method is unlikely to work as well at lower resolution, since the order parameter will be higher [20]. The wider applicability of the technique therefore needs further investigation.

ACKNOWLEDGMENT

The authors would like to thank JAXA for the PALSAR-2 data, and Dr. Shimada in particular.

REFERENCES

[1] P. A. Wright, S. Quegan, N. S. Wheadon, and C. D. Hall, "Faraday rotation effects on L-band spaceborne SAR data," *IEEE Trans. Geosci Remote Sens.*, vol. 41, no. 12, pp. 2735–2744, Dec. 2003.

[2] S. Quegan and I. Rhodes, "Problems in the linear distortion model for polarimetric calibration," in *Proc. CEOS Calibration Workshop*, 1993, pp. 127–132, paper WPP-048.

[3] F. Meyer, R. Bamler, N. Jakowski, and T. Fritz, "The potential of low-frequency SAR systems for mapping ionospheric TEC distributions," *IEEE Geosci. Remote Sens. Lett.*, vol. 3, no. 4, pp. 560–564, Oct. 2006.

[4] D. P. Belcher, "Theoretical limits on SAR imposed by the ionosphere," *IET Radar, Sonar Navigat.*, vol. 2, no. 6, pp. 435–448, Dec. 2008, doi: 10.1049/iet-rsn:20070188.

[5] D. P. Belcher and P. S. Cannon, "Amplitude scintillation effects on SAR," *IET Radar, Sonar Navigat.*, vol. 8, no. 6, pp. 658–666, 2014, doi: 10.1049/iet-rsn.2013.0168.

[6] F. J. Meyer, K. Chotoo, S. D. Chotoo, B. D. Huxtable, and C. S. Carrano, "The influence of equatorial scintillation on L-band SAR image quality and phase," *IEEE Trans. Geosci. Remote Sens.*, vol. 54, no. 2, pp. 869–880, Feb. 2016.

[7] D. P. Belcher and P. S. Cannon, "Ionospheric effects on synthetic aperture radar (SAR) clutter statistics," *IET Radar, Sonar Navigat.*, vol. 7, pp. 1004–1011, Dec. 2013, doi: 10.1049/iet-rsn.2012.0227.

[8] D. P. Belcher and N. C. Rogers, "Theory and simulation of ionospheric effects on synthetic aperture radar," *IET Radar, Sonar Navigat.*, vol. 3, pp. 541–551, Oct. 2009, doi: 10.1049/iet-rsn.2008.0205.

[9] D. P. Belcher, P. S. Cannon, and A. Gustavsson, "The Ascension Island experiment: Measurement of ionospheric scintillation effects on PALSAR-2," in *Proc. Int. Geosci. Remote Sens. Symp. (IGARSS)*, Milan, Italy, Jul. 2015, pp. 3191–3194, doi: 10.1109/IGARSS.2015.7326496.

[10] C. R. Mannix, D. P. Belcher, and P. S. Cannon, "Measurement of ionospheric scintillation parameters from SAR images using corner reflectors," *IEEE Trans. Geosci. Remote Sens.*, to be published.

[11] C. Oliver and S. Quegan, *Understanding Synthetic Aperture Radar Images*. Raleigh, NC, USA: SciTech Publishing Inc, 2004.

[12] Y. Kankaku, S. Suzuki, and Y. Osawa, "ALOS-2 mission and development status," in *Proc. IEEE Geosci. Remote Sens. Symp. (IGARSS)*, Melbourne, VIC, Australia, Jul. 2013, pp. 2396–2399.

[13] C. L. Rino, "On the application of phase screen models to the interpretation of ionospheric scintillation data," *Radio Sci.*, vol. 17, no. 4, pp. 855–867, 1982.

[14] E. J. Fremouw and J. A. Secan, "Modeling and scientific application of scintillation results," *Radio Sci.*, vol. 19, no. 3, pp. 687–694, 1984.

[15] K. D. Ward, "Compound representation of high resolution sea clutter," *Electron. Lett.*, vol. 17, no. 16, pp. 561–563, 1981.

[16] C. J. Oliver, "The representation of correlated clutter textures in coherent images," *Inverse Problems*, vol. 4, no. 3, pp. 843–866, 1988.

[17] D. Blacknell and R. J. A. Tough, "Parameter estimation for the K-distribution based on [z log(z)]," *IEE Proc.-Radar, Sonar Navigat.*, vol. 148, no. 6, pp. 309–312, Dec. 2001, doi: 10.1049/ip-rsn:20010720.

[18] C. R. Mannix, "Measuring and modelling the impact of the ionosphere on space based synthetic aperture radars," Ph.D. dissertation, College Eng. Phys. Sci., Univ. Birmingham, Birmingham, U.K., 2016.

[19] D. P. Belcher and P. S. Cannon, "Errata to 'Ionospheric effects on synthetic aperture radar (SAR) clutter statistics,'" *IET Proc.-Radar, Sonar Navigat.*, vol. 8, no. 1, p. 71, 2014.

[20] A. P. Blake, D. Blacknell, and C. J. Oliver, "SAR clutter analysis and its resolution dependence," in *Proc. Radar*, 1997, pp. 124–128, doi: 10.1049/cp:19971645.

David P. Belcher received the B.Sc. degree in physics from Kings College London, London, U.K., and the Ph.D. degree from the University College London, London, in 1997.

He joined the Royal Signals and Radar Establishment (RSRE), Great Malvern, U.K., in 1989. At RSRE (later called DRA and DERA) he worked on high-resolution synthetic aperture radar (SAR) processing, including image distortion, inertial sensors, spotlight mode, and autofocus. He managed the Airborne Low-Frequency SAR program at DERA and was promoted as a Senior Scientist in 1998. He joined Dstl, Great Malvern, in 2001, where he led the UK Radar Team for several international collaborative projects in system-level space-based SAR and MTI, and also became a Dstl Associate Fellow in 2005, individually funded for his work on space-based low-frequency SAR. He joined the University of Birmingham, Birmingham, U.K., as a Co-Investigator in 2011, where he developed a theoretical description of the effects of ionospheric turbulence on space-based SAR, and designed an experiement to test his theory.

Christopher R. Mannix received the M.Sc. degree in physics and the Ph.D. degree in electronic, electrical and systems engineering from the University of Birmingham, Birmingham, U.K., in 2012 and 2016, respectively.

His research interests include the effects of the ionosphere on radar and navigation systems, as well as the use of synthetic aperture radar systems as an ionospheric measurement tool.

Paul S. Cannon received the B.Sc. degree in physics, the M.Sc. degree in electronics, and the Ph.D. degree in space radio physics from the University of Southampton, Southampton, U.K., in 1975, 1976, and 1981, respectively.

From 1979 to 1981, he was a Satellite Communications Engineer with Marconi Space and Defence Systems, Farnborough, U.K. During 1981–2001, he was a Research Scientist with the UK Ministry of Defence, Great Malvern, U.K. In 2001, his laboratory was privatized to become a part of QinetiQ plc, Great Malvern. In 2013, he joined the University of Birmingham, Birmingham, U.K., as a Professor of Radio Science and Systems. He has made numerous personal and team contributions and his papers include those addressing ionospheric modification, high-frequency communications and radars, meteor scatter communications, and space radars. His research interests include radio propagation and the radio environment impact on communications, radar and navigation systems.

Dr. Cannon is a fellow of the Royal Academy of Engineering. He was appointed to the Office of the Order of the British Empire by Her Majesty the Queen in 2014. He serves on the Government Advisory Committees. He has been an Expert Witness to a Parliamentary Select Committee and has supported the Prime Minister's Committee on Science and Technology. He is currently the President of the International Union of Radio Science.